EACWE2022

8th European-African Conference on Wind Engineering
20-23 September 2022 | Bucharest, Romania

Solar trackers analysis: a parametric study to evaluate aeroelastic effects inside a photovoltaic park array

Giorgio Frontini[1*)], Filippo Calamelli[2)], Sara Muggiasca[3)], Tommaso Argentini[4)], Marco Belloli[5)]

1) Politecnico di Milano, Italy, giorgio.frontini@polimi.it
2) Politecnico di Milano, Italy, filippo.calamelli@polimi.it
3) Politecnico di Milano, Italy, sara.muggiasca@polimi.it
4) Politecnico di Milano, Italy, tommaso.argentini@polimi.it
5) Politecnico di Milano, Italy, marco.belloli@polimi.it

ABSTRACT: In current design practice, simplified methods for the dimensioning of photovoltaic trackers are largely used. These methods usually neglect the aeroelastic effect: several studies, however, observed that for such structures this contribution may be critical for some configurations, and so it should be accounted for an accurate response evaluation. In the present article a parametric study for varying wind speed, pitch angle, exposure, ground cover ratio, damping and position in the array is carried out with the objective to assess when the simplified approaches are able to characterize the trackers response, and when their use leads to wrong estimations.

Keywords: Solar arrays, Single axis tracker, Wind tunnel test, Wind loads, Aeroelasticity

1. INTRODUCTION

Photovoltaic (PV) trackers are structures characterized by a longitudinal torsional tube supporting a large number of solar panel modules; one or multiple motor drives are installed in order to change the panel orientation and track the Sun during the course of the day. Typically, these objects are installed in vast open-areas in order to obtain the best ratio of converted energy per unit of terrain area; in addition, to optimize the return of investment, producers of these structures tend to minimize the amount of material adopted in the assembly. Due to the savings in production costs, the resulting structures are lightweight and consequently very susceptible to the turbulent wind that acts on their large surfaces. The response to the aforementioned wind actions is characterized by a static component, associated to the mean wind speed, and by a dynamic component, mainly due to resonant response, associated to the presence of time-varying loads induced by turbulence. Moreover, due to the particular geometry of the panels, which is similar to a flat plate, for some inclination angles (conventionally called also pitch or tilt angles) aeroelastic effects arise due to the incoming mean wind speed. It follows that the resulting dynamic response of the structure is influenced by the aerodynamic stiffness and damping.

In the current design practice, Equivalent Static Wind Loads (ESWLs) (Davenport, 1967); Holmes, 1988; Chen and Kareem, 2001) are usually adopted: a set of static loads is applied on the structure in order to reproduce the extreme effects of the dynamic wind loads. The dimensioning ESWLs for photovoltaic trackers are usually obtained by means of simplified approaches which involves the adoption of synthetic information provided by the implementation of so-called Dynamic Amplification Factors (DAF) (Browne et al., 2020). With this approach, the dynamic effects are estimated in a simplified way; in fact, only the spectrum of the acting pressure (or moment) and the modal characteristics of the tracker are required as inputs. This simplified formulation, however, brings shortcomings which limit its scope of application. Firstly, in the evaluation of the coefficients, the

*) *Corresponding author*

dynamic response of the tracker is accounted for only a single frequency: typically, the first torsional mode of the structure, that is the one most excited by the incoming wind. All modes higher than the first are thus neglected. Second, the DAF approach is valid only if the tracker is not susceptible to aeroelastic effects and torsional instabilities. Real-life experience, however, shows that, especially for lower pitch angles (≤ 30°), at typical design mean wind speed, these constructions are often unstable. It follows that applying the results of the simplified DAF approach without considering the actual aeroelastic contribution, can lead to design actions on the unsafe-side. For this purpose, a different design procedure, able to account for the self-excited response of the tracker, has to be adopted. As a reference for the study here presented, Taylor and Browne (2020) illustrated how it is possible to combine the results of rigid-model and sectional model wind tunnel tests in order to evaluate the complete aerodynamic response of a structure in a so-called "hybrid method".

In the present paper, the time histories of the structural responses of a tracker are evaluated both considering and neglecting the self-excited response. The two sets of results are then compared in a parametric study, in which the mean wind velocity, the ground cover ratio (GCR), the tracker pitch angle, the exposure angle and the structural damping have been varied. After a brief description of the aforementioned hybrid method, implemented for the analysis, the results of a case study, obtained by loading a numerical model with pressure distribution measured in a set of experimental tests, are presented. For each scenario a comparison is made between the case in which the self-excited response of the tracker is respectively accounted for and neglected. These comparisons will show when simplified formulations are able to provide responses in accordance with the observed aeroelastic structural behaviour and when, instead, such procedures should be avoided and a more refined study of the problem should be carried out instead.

2. PROCEDURE

2.1 Response evaluation

The structural response of the solar tracker can be characterized by the classical dynamic equilibrium. Generally, the structural properties are derived from a finite element model, while the forcing term is evaluated with experimental tests in wind tunnel facilities. In the modelling of the equation, the acting loads can be dived into a mean static component and a buffeting component, both evaluated with tests on scaled rigid models of the entire park. From the integration of the governing equation, the structural displacements are evaluated by summing the mean static and the dynamic components.

If aeroelastic effects are not negligible, the forcing term in the dynamic equilibrium is characterized by also a self-excited contribution: tests on a suspended sectional model, aimed at the evaluation of flutter derivatives, are required for the evaluation of this term. Since trackers are usually susceptible to wind induced effects only in correspondence of the first torsional mode, the computations can be limited to a characterization of the torsional behaviour with flutter derivatives a_2^* and a_3^*. With the additional information given by these two terms, the dynamic equilibrium can be rewritten to account for the aeroelastic contribution on the torsional moment, identified as M_{aero}, which is directly related to the structural response in term of rotation angle θ and angular velocity $\dot{\theta}$. Considering the first mode in a modal reference system, the Lagrangian component of the aeroelastic forces, is written as:

$$Q_{\text{aero,1}} = \int_L \varphi_1 M_{\text{aero}} dx = \frac{1}{2}\rho U^2 B^2 \int_L \varphi_1^2 a_3^* dx \cdot q_1 - \frac{1}{2}\rho U B^3 \int_L \varphi_1^2 a_2^* dx \cdot \dot{q}_1 = \mathrm{K}_{\text{aero,1}} \cdot q_1 - \mathrm{R}_{\text{aero,1}} \cdot \dot{q}_1 \quad (1)$$

In which φ_1 is the deformed shape of the first (torsional) mode, ρ is the air density, B is the tracker chord length, L is the tracker length and U is the normal mean wind speed at the torque tube height. a_3^* and a_2^* are the flutter derivatives associated to the aerodynamic stiffness $\mathrm{K}_{\text{aero,1}}$ and damping $\mathrm{R}_{\text{aero,1}}$ respectively. The equation of motion can then be expressed in a modal reference system as:

$$\mathrm{M}_{\text{str,1}}\ddot{q}_1 + \left(\mathrm{R}_{\text{str,1}} + \mathrm{R}_{\text{aero,1}}\right)\dot{q}_1 + \left(\mathrm{K}_{\text{str,1}} - \mathrm{K}_{\text{aero,1}}\right)q_1 = Q_{\text{buff,1}} \quad (2)$$

Where, with respect to the first mode in a modal reference system q_1 is the modal coordinate, $\mathrm{M}_{\mathrm{str},1}$, $\mathrm{R}_{\mathrm{str},1}$ and $\mathrm{K}_{\mathrm{str},1}$ are respectively the contributions to the modal mass, damping and stiffness, and $Q_{\mathrm{buff},1}$ is the generalized Lagrangian forcing vector of the acting buffeting loads.

3. CASE STUDY

3.1 Definition of the numerical finite element (FE) model

To perform the study object of this paper, a FE model of a typical photovoltaic tracker has been developed taking as a full-scale reference a generic 2x45 PV tracker, characterized by a tracker length of 45m, a chord length of 4m and a torque tube at 2m above ground. Regarding the posts, a motorized post is present in the central section of the tracker.

3.2 Experimental wind-tunnel tests

For the present study two series of experimental tests were carried out at Politecnico di Milano Wind Tunnel. The first set, carried out on rigid-scaled model for different parameters, such as exposure angle, pitch angles and spacing between adjacent rows, was aimed at the evaluation of the acting pressure distribution on the solar tracker. The second set, performed on a suspended sectional model, was aimed at the tracker aeroelastic characterisation for different wind velocities and pitch angles. From the sectional model tests, a preliminary analysis can be already performed on the computed flutter derivatives: such data, in fact, allow the designer to have some insight about the effects of the aeroelastic contribution. Since a negative total stiffness is associated to structural-static instabilities and a negative total damping is associated to aerodynamic instabilities, from previous Eq. (2) it is possible to derive the two inequalities $(\mathrm{R}_{\mathrm{str},1} + \mathrm{R}_{\mathrm{aero},1}) < 0$ and $(\mathrm{K}_{\mathrm{str},1} - \mathrm{K}_{\mathrm{aero},1}) < 0$ in order to assess for which range of wind velocity and pitch angles the system is unstable. Combining the two inequalities, it is also possible to identify, in an approximate way, the stable and unstable regions of the studied tracker, as shown in Figure 1.

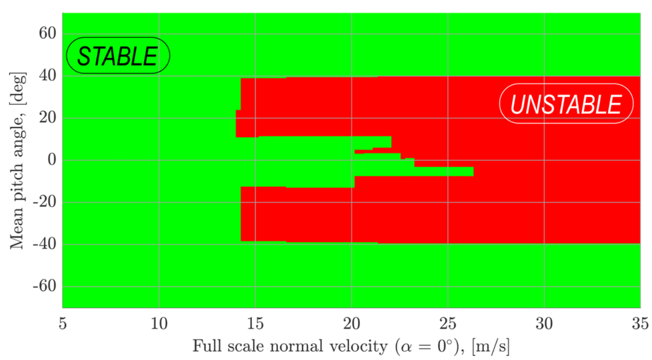

Figure 1. Stability map of the tracker

3.3 Numerical computations

The numerical simulations of the tracker response were performed combining the structural information gathered from the FE model and assuming values of the critical damping ranging from 2% to 10%. The forcing loads were inferred from the rigid scale test, while the flutter derivatives, obtained from the sectional model, were implemented for the characterization of the self-excited response in the hybrid approach. From the structural displacements obtained by solving the dynamic equilibrium, internal actions and stresses can be evaluated by exploiting the local structural stiffness. In the presented examples the analyses were carried out in terms of the Von Mises stress acting in the torque tube. To identify the design values from the time history of the responses, a statistical method (more specifically the Gumbel method) has been implemented.

In Figure 2 the influence of some parameters is illustrated: on the abscissas is reported the torque tube location, while on the ordinate is reported the Von Mises stresses expressed in MPa; the response considering self-excited response is reported with a red line, while with the blue line are depicted the results obtained neglecting this contribution. All results are evaluated assuming a full-scale mean wind speed at torque tube height of 15 m/s.

In Figure 2a, as a reference case, is reported the response associated to the first row of the solar array (R1), considering 10% of damping and a pitch angle of 30°. In Figure 2b is depicted the effect of the variation of the pitch angle: changing from 30°to 60°, it can be observed that, for the higher pitch angles the system is stable and the self-excited response is negligible. In Figure 2c the response of the second row (R2) of the solar array is plotted. Compared against the first row (R1) it is possible to observe that, due to the reduction in wind speed given by the shielding effect of the perimetral trackers, the self-excited contribution is much lower, as the two curves are quite identical. Finally, in Figure 2d is depicted the effect of a reduction in the structural damping. As it can be seen, the tracker is reaching unstable conditions and its response tends to diverge: in this scenario the simplified method is not able to predict the actual tracker response.

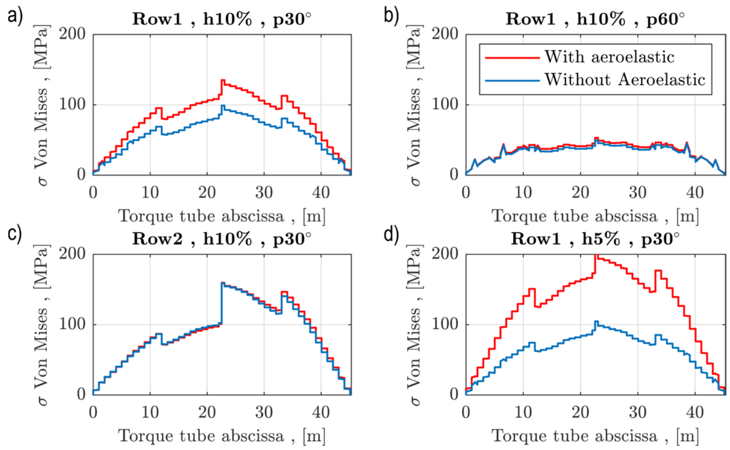

Figure 2. Effects of the variation of some parameters in the results:
a) reference case, b) different pitch angle, c) different row in the array, d) different structural damping

4. CONCLUSIONS

The relevance of the aerodynamic effects depends on the induced variation of the total stiffness and damping matrices. From the results reported in Figure 2 it is possible to observe that, generally, when the aeroelastic effects are relevant, the structural response tends to be much worse with respect to the case of neglecting them. This relevance is dependent on the pitch angle and the wind speed observed by the tracker. For higher pitch angles, and for trackers protected from the incoming wind by the perimetral trackers in a PV park, the self-excited response is close to be negligible. For lower pitch angles and perimetral trackers this contribution is more relevant and should be accounted for; in this case, the use of simplified approaches could lead to severe underestimation in the design. This observation can be also derived by the colourmap of Figure 1, were, in an approximated way, a designer could get an idea regarding which ranges of pitch angles and wind velocities are problematic for the stability of the structures under investigation.

Acknowledgements
The results presented in this research were obtained in the development of a project founded by ENEL S.p.A. The authors would like to acknowledge and thank the company for the questions that initiated the development of the presented analysis and the provided technical knowledge.

References

Browne M.T.L., Taylor Z.J., Li S., Gamble S. (2020), A wind load design method for ground-mounted multi-row solar arrays based on a compilation of wind tunnel experiments, *Journal of Wind Engineering and Industrial Aerodynamics*

Chen X., Kareem A. (2001), Equivalent static wind loads for buffeting response of bridges, *Journal of Structural Engineering*

Davenport A. G. (1967), Gust loading factors, *Journal of the Structural Division*

Holmes J. D. (1988), Distribution of peak wind loads on a low-rise building, *Journal of Wind Engineering and Industrial Aerodynamics*

Taylor Z.J., Browne M.T.L. (2020), Hybrid pressure integration and buffeting analysis for multi-row wind loading in an array of single-axis trackers, *Journal of Wind Engineering and Industrial Aerodynamics*

EACWE2022

8th European-African Conference on Wind Engineering
20-23 September 2022 | Bucharest, Romania

Multi-mode high-order wind-induced vibration control on ultra-long stay cables by using a novel dual damper system

Yafei Wang[1*)], James BrownJohn[2)], ZhengQing Chen[3)]

1) Hunan University, China and University of Exeter, the United Kingdom, y.wang15@exeter.ac.uk
2) University of Exeter, the United Kingdom, j.brownjohn@exeter.ac.uk
3) Hunan University, China, zqchen@hnu.edu.cn

ABSTRACT: Multi-mode high-order wind-induced vibration of the ultra-long stay cables has been observed on a super-span cable-stayed bridge named Sutong. The field vibration monitoring system exhibits the modal order of rain-wind-induced vibration of the super-long stay cables ranges from 11th to 17th, and the vortex-induced vibration spreads over 9th -26th. A new damping coefficient design scheme was deduced to suppress such abnormal wind-induced vibration, and a novel damper system was developed and installed on the test stay cable. Finally, one-year more field monitoring shows that the multi-mode high-order vibration responses of the monitored stay cables are effectively suppressed, and this paper is supposed to provide a reference to practical super-long stay cables wind-induced vibration control.

Keywords: stay cable, wind-induced vibration, damping system design, field monitoring.

1. INTRODUCTION

It is generally believed that rain-wind-induced vibration (RWIV) is the most harmful, and vortex-induced vibration (VIV) is the most common and frequently occurring vibration. Besides, based on the published literature and journals, it is generally believed that RWIV and VIV happen in the first several modes, and engineers always set the first five orders as the aim of the cable vibration control.

However, with the further increase of the main span of cable-stayed bridges, multi-mode high-order wind-induced vibrations involving the in-plane and out-of-plane response of stay cables were observed on some cable-stayed bridges. Ge and Chen (2019) observed the high-order VIV with a frequency ranging from 9.5 to 10.0 Hz on some stay cables of the Sutong Bridge (STB) in Jiangsu, China. Liu et al. (2021) observed high-order wind-induced vibration on cables of the JiaYu Bridge in Hubei, China. In other words, for ultra-long stay cables, the common first-several-modes-aimed damping scheme may be no longer suitable. Consequently, this study aims at developing a new damping system for high-order multi-mode vibration control of the ultra-long stay cables.

2. NEW VIBRATION RESPONSE

2.1 The STB and the VMS

The STB is a cable-stayed bridge with a main span of 1088 m and a streamlined steel closed-box girder, which was completed and opened to traffic in 2008, and the most extended stay cable length of the bridge is 567.77 m.

In order to investigate the wind-induced vibration characteristics of the ultra-long stay cables, a vibration monitoring system (VMS) was established on the STB. Figure. 1 describes the monitored stay cables and the position of the sensors.

*) *Corresponding author*

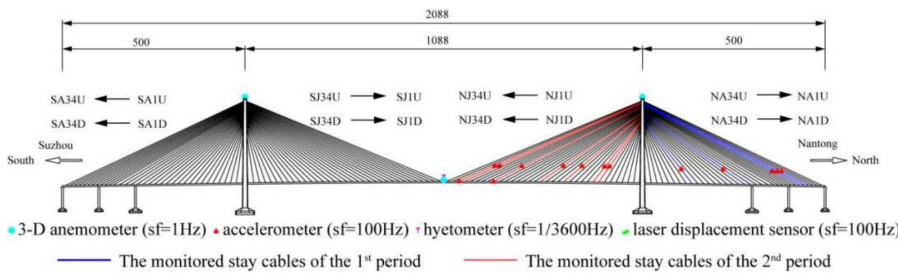

Figure. 1 Schematic diagram of the stay cables and the original damper system of the STB (a) The monitored stay cables and the sensors of the STB (unit: m)

2.2 New vibration response

Figure 2a and Figure 2b shows the 1-minute acceleration root mean square (RMS) of the stay cable NA30U during the monitoring period of three months. The stay cable performs severe vibration for both the in-plane vibration and out-of-plane vibration, and the maximum in-plane and out-of-plane 1-minute acceleration RMS are 1.217g and 1.337g, respectively. Figure 2c and Figure 2d show the 10-minute average power spectrum density (APSD) of the acceleration response of the stay cable NA30U. The fundamental frequency of the stay cable NA30U is 0.261 Hz, so that the in-plane modal order spreads from 9th to 47th, and the out-of-plane modal order concentrates between 8th to 16th and 46th to 47th.

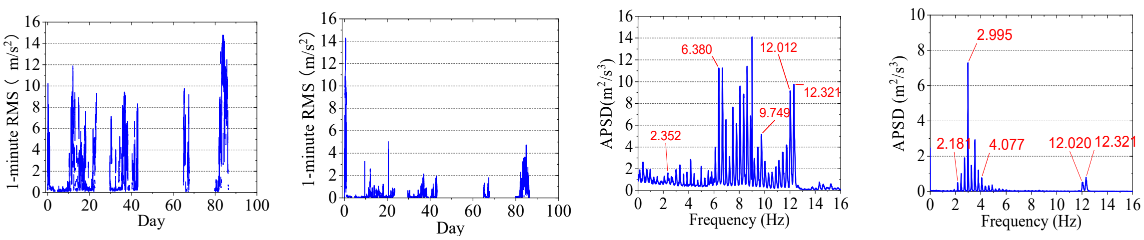

(a) In-plane RMS (b) Out-of-plane RMS (c) In-plane APSD (d) Out-of-plane APSD

Figure 2. 1-minute acceleration RMS of cable NA30U controlled by the original damper system (Note: There exists data missing due to the accelerometer problems).

The above vibration responses are quite different from the traditional opinions, so in this study, they are classified into rain-wind-induced vibration (RWIV), vortex-induced vibration (VIV) and Micro-vibration (MV), as shown in Table 1.

Table 1. Characteristics of the three vibration responses of the stay cable NA30U

Vibration types	Frequency band (Hz)	Dominant vibration direction	Maximum out-of-plane RMS (m/s^2)	Maximum in-plane RMS (m/s^2)
RWIV	2.18 - 4.1	out-of-plane	14.27	5.66
VIV	2.3 - 12.3	in-plane	6.03	16.14
MV	< 6	in-plane	0.32	0.99

3. NEW DAMPING SCHEME AND THE EFFECTS

3.1 New damping ratio design scheme

The commonly used damping scheme for stay cable is

$$\zeta_k = \zeta_1 \geq \zeta_{\min}, \tag{1}$$

in which ζ_{min} denotes the required minimum damping ratio, and ζ_k, ζ_1 denotes the damping ratio of the highest control mode and the first mode of the stay cable. In order to mitigate the multi-mode high-order VIV and RWIV with out-of-plane and in-plane vibration involved, a new damping coefficient design method is proposed, as shown in Equation. (2).

$$\zeta_3 \geq \zeta_{\min} \tag{2}$$

The new damping scheme means that this study gives up the first-two order vibration control to broaden the vibration control range and improve the high-order modal damping ratio. Figure 3 shows an example of the difference between the modal control ranges of the two different damping optimization schemes.

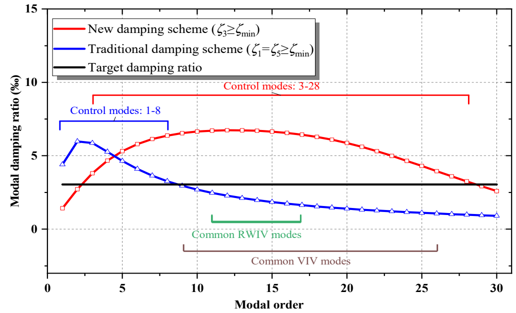

Figure 3. Comparison of the modal control ranges of the two different optimization schemes. (Note: the efficiency coefficient of the damper is considered to be 0.5. Target damping ratio=3.25‰)

3.2 New damper system

A practical novel eddy current damper system (ECDS) is developed and installed on the stay cables for the simultaneous in-plane and out-of-plane vibration control, as shown in the Figure 4a. Figure 4b shows the original damper system as the comparison.

(a) Eddy current damper system (ECDS), (b) Original stay cable damper system

Figure 4. The comparison of the two different damper system

3.3 Field measurements and validation

Field monitoring results are calculated and plotted in Figure 5. It can be seen that the new damping scheme achieved good effects.

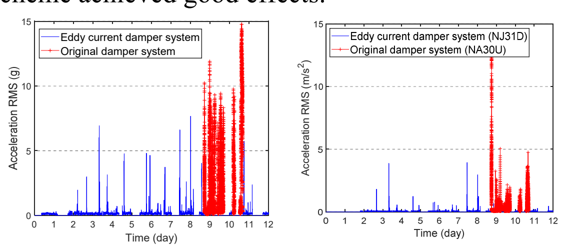

(a) Out-of-plane acceleration (b) In-plane acceleration (c) Out-of-plane APSD (d) In-plane APSD

Figure 5. Comparison of the 1-minute RMS acceleration and every-10-minute APSD between the two different damping systems ('APSD' denotes the average power spectrum density)

4. IMPROVEMENT IN PHASE Ⅱ

It can be seen from Figure 5c and Figure 5d that there are still some super high-order modal vibrations of about 10 Hz to 12 Hz after the above damping optimization, which is called stagnation point effect-induced vibration. Consequently, the improvement in Phase Ⅱ aims at the narrow band super-high-order vibration control. Stockbridge Damper is introduced and used here, as shown in Figure 6. Field monitoring results are plotted in Figure 7.

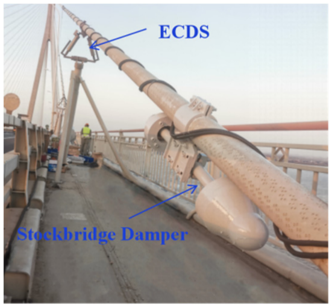

Figure 6. ECDS+ Stockbridge double dampers system

Figure 7. Comparison of the every-10-minute APSD

5. CONCLUSIONS

The conclusions can be drawn as flows:

(1) For ultra-long stay cables with a length of more than 450 m, the wind-induced vibration mode order can be up to more than 40^{th}. So that the commonly used first-several-aimed damping scheme is no longer suitable for such kind of stay cable vibration control.

(2) The new damping scheme in this study by giving up the first-two order vibration control, broadening the vibration control range and improving the high-order modal damping ratio can be effective on multi-mode high-order vibration for ultra-long stay cables.

(3) ECDS can be used to control the wind-induced stay cable vibration with in-plane and out-of-plane vibration involved.

(4) A single damper system used on ultra-long stay cables can cause additional stagnation point effect-induced vibration. However, ECDS and Stockbridge double dampers system can effectively suppress nearly all the modal vibration of ultra-long stay cables.

References

Chen L, et al. (2020). A comparative study of multi-mode cable vibration control using viscous and viscoelastic dampers through field tests on the Sutong Bridge. Engineering Structures.

Chen W-L, et al. (2015). An experimental investigation on vortex-induced vibration of a flexible inclined cable under a shear flow. Journal of Fluids and Structures.

Chen ZQ, et al. (2004). MR damping system for mitigating wind-rain induced vibration on Dongting Lake Cable-Stayed Bridge. Wind & structures. 2004 Sep 1;7(5):293-304.

Chen ZQ. (2014). An axial eddy current damper that rotates by the outer cup. CN 104265818 A. (in Chinese)

Chen ZQ, et al. (2014). An axial eddy current damper based on the screw. CN 103821861 A. (in Chinese)

D'Auteuil A, et al. (2020). A new large-scale dynamic rig to evaluate rain-wind induced vibrations on stay cables: Design and commissioning. Journal of Wind Engineering & Industrial Aerodynamics. 2020

Liu Z, et al. (2020). Experimental study on high-mode vortex-induced vibration of stay cable and its aerodynamic countermeasures. Journal of Fluids and Structures.

Liu M, Yang W, et al. (2019). Experimental Investigation on Vortex-Induced Vibration Mitigation of Stay Cables in Long-Span Bridges Equipped with Damped Crossties. Journal of Aerospace Engineering.

Pacheco BM, et al. (1993). Estimation curve for modal damping in stay cables with viscous damper. Journal of Structural Engineering. Jun;119(6):1961-79.

Yangchen D, et al. (2021). Experimental investigation on wake-induced vibrations of the hangers of suspension bridges based on three-dimensional elastic test model. Engineering Structures.